The Journal of Microbiology (2011) Vol. 49, No. 5, pp. 797-802
DOI 10.1007/s12275-011-0487-5

Biochemical Properties and Physiological Roles of NADP-Dependent Malic Enzyme in *Escherichia coli*

Baojuan Wang[1†], Peng Wang[1†], Enxia Zheng[1†], Xiangxian Chen[1], Hanjun Zhao[2], Ping Song[1], Ruirui Su[1], Xiaoning Li[3], and Guoping Zhu[1*]

[1]*Key Laboratory of Molecular Evolution and Biodiversity and Institute of Molecular Biology and Biotechnology, Anhui Normal University, Wuhu 241000, P. R. China*
[2]*The Clinical Laboratory of Wuhu Second People's Hospital, Wuhu 241000, P. R. China*
[3]*Yijishan Hospital of Wannan Medical College, Wuhu 241000, P. R. China*

(Received November 29, 2010 / Accepted April 25, 2011)

Malic enzymes catalyze the reversible oxidative decarboxylation of L-malate using NAD(P)$^+$ as a cofactor. NADP-dependent malic enzyme (MaeB) from *Escherichia coli* MG1655 was expressed and purified as a fusion protein. The molecular weight of MaeB was about 83 kDa, as determined by SDS-PAGE. The recombinant MaeB showed a maximum activity at pH 7.8 and 46°C. MaeB activity was dependent on the presence of Mn^{2+} but was strongly inhibited by Zn^{2+}. In order to understand the physiological roles, recombinant *E. coli* strains (*icd*^{NADP}/Δ*maeB* and *icd*^{NAD}/Δ*maeB*) containing NADP-dependent isocitrate dehydrogenase (IDH), or engineered NAD-dependent IDH with the deletion of the *maeB* gene, were constructed using homologous recombination. During growth on acetate, *icd*^{NAD}/Δ*maeB* grew poorly, having a growth rate only 60% that of the wild-type strain (*icd*^{NADP}). Furthermore, *icd*^{NADP}/Δ*maeB* exhibited a 2-fold greater adaptability to acetate than *icd*^{NAD}/Δ*maeB*, which may be explained by more NADPH production for biosynthesis in *icd*^{NADP}/Δ*maeB* due to its NADP-dependent IDH. These results indicated that MaeB was important for NADPH production for bacterial growth on acetate. We also observed that MaeB activity was significantly enhanced (7.83-fold) in *icd*^{NAD}, which was about 3-fold higher than that in *icd*^{NADP}, when switching from glucose to acetate. The marked increase of MaeB activity was probably induced by the shortage of NADPH in *icd*^{NAD}. Evidently, MaeB contributed to the NADPH generation needed for bacterial growth on two carbon compounds.

***Keywords*:** NADP-dependent malic enzyme, biochemical property, homologous recombination, growth rate, NADPH

Malic enzymes (MEs) are important malate metabolizing enzymes, which catalyze the reversible oxidative decarboxylation of L-malate coupled with the reduction of dinucleotide cofactor NAD(P)$^+$ to yield pyruvate and CO_2 (Chang and Tong, 2003; Detarsio *et al*., 2004; Bologna *et al*., 2007). MEs are widely distributed in all three domains of life and involved in a great number of metabolic pathways, due to the key metabolites derived from ME reactions in central carbon and energy metabolism (Lance and Rustin, 1984; Song *et al.*, 2001). These include: carbon fixation in tropical C4 plants, lipogenic NADPH production in fungi and animals, energy production in rapidly proliferating tissues by the mitochondrial isoform (Doležal *et al.*, 2004; Lerondel *et al.*, 2006), and the ability to metabolize extracellular malic acid (Seo *et al*., 2007).

MEs can be divided into two major protein types based on their cofactor preference, NAD-dependent ME (NAD-ME) and NADP-dependent ME (NADP-ME) (Murai *et al*., 1971; Fukuda *et al*., 2005; Wheeler *et al*., 2005). Eukaryotic malic enzymes have been characterized from a wide variety of sources and most are homotetramers with subunits of 65.4-71 kDa each (Mitsch *et al*., 1998). MEs may be further classified into three groups in eukaryotic organisms: the first group (EC 1.1.1.38) preferentially utilizes NAD^+ as a cofactor and catalyzes oxaloacetate (OAA) decarboxylation; the second group (EC 1.1.1.39) is made up of NAD-dependent enzymes exclusively located in mitochondria, which are not able to decarboxylate OAA; the third group (EC 1.1.1.40) consists of NADP-dependent proteins that can catalyze the decarboxylation of both malate and OAA in the cytosol, chloroplasts, and mitochondria (Lerondel *et al*., 2006; Bologna *et al*., 2007).

The prokaryotic malic enzymes described so far are fewer in number and more varied in structure than their eukaryotic counterparts (Lerondel *et al*., 2006; Bologna *et al*., 2007). For example, the Gram-negative bacterium *Rhizobium meliloti* contains two distinct malic enzymes with unusually high subunit molecular weight of about 82 kDa (Voegele *et al*., 1999). Additionally, a 208 kDa NADP-dependent tetramer and a 680 kDa decamer have been found in two separate *Pseudomonas* species (Garrido-Pertierra *et al.*, 1983; Suye *et al.*, 1992). MEs from three thermophilic organisms have also been purified, a NADP-dependent tetramer from *Clostridium thermocellum* (Lamed and Zeikus, 1981), a NADP-dependent dimer from *Sulfolobus solfataricus* (Bartolucci *et al*., 1987) and a tetramer utilizing both cofactors from *Bacillus stearothermophilus*

† These authors contributed equally to this work.
* For correspondence. E-mail: gpz1996@yahoo.com; Tel. and Fax: +86-553-3883592

Table 1. Primer sequences and genetic background of strains used in this study

Names	Sequences or information about genetic background
Primers	Primer sequences for *maeB* cloning (5′→3′)
P1	GATTGGCCATGGATGACCAGTTAAACAAAGTG-3′ (*Nco*I site underlined)
P2	GTGTCTCGAGTTAATGATGATGATGATGATGCAGCGGTTGGGTTT-3′ (*Xho*I site underlined)
	Primer sequences for *maeB* deletion (5′→3′)
D1	TTGTGAACGTTACGTGAAAGGAACAACCAAATGGATGACCAGTTAAAACAGTGTAGGCTGGAGCTGCTTC
D2	GGTTTCGCCACACCCATCAGCACCGGGCCGACAGTCACACCTTCCGAGCTAGTGATAAGCTGTCAAACAT
	Primer sequences for confirmation of *maeB* deletion (5′→3′)
C1	AATGCCTTCAGACAGTTTTTCTACCGCC
C2	ACATCAGTGTTATAGGATTATTACC
C3	TCCAGCTCGGAAGGTGTGACTGTCGG
C4	CAACGCCCGCTTTGATCTGCAAGCCCAGTTTC
C5	AGGCGGCCCTGCTCGTCAATAAAC
Strains	Genetic background of wild-type and recombinant strains
icd^{NADP}	Genotype: F^-, lambda$^-$, rph-1, icd^{NADP}; Phenotype: *E. coli* MG1655 contains NADP-dependent IDH (wild type)
icd^{NAD}	Genotype: F^-, lambda$^-$, rph-1, icd^{NAD}; Phenotype: *E. coli* MG1655 contains engineered NAD-dependent IDH
icd^{NADP}/Δ*maeB*	Genotype: F^-, lambda$^-$, rph-1, icd^{NADP}, *maeB*$^-$; Phenotype: *E. coli* MG1655 contains NADP-dependent IDH with *maeB* deletion
icd^{NAD}/Δ*maeB*	Genotype: F^-, lambda$^-$, rph-1, icd^{NAD}, *maeB*$^-$; Phenotype: *E.* coli MG1655 contains engineered NAD-dependent IDH with *maeB* deletion

(Kobayashi *et al*., 1989). Most recently, smaller MEs of approximately 40 kDa per subunit were characterized from *Corynebacterium glutamicum* (Gourdon *et al*., 2000) and *Lactococcus lactis* (Sender *et al*., 2004). Interestingly, *Bacillus subtilis* has four paralogous malic enzyme isoforms (45-60 kDa): MalS, MleA, and MaeA which exhibited 4- to 90-fold higher activities with NAD^+ than with $NADP^+$ as coenzyme, and YtsJ which, in contrast, had 70-fold higher activity with $NADP^+$ than with NAD^+ as coenzyme (Lerondel *et al*., 2006).

In *E. coli*, MaeA (or SfcA) and MaeB (encoded by *maeB*) are NAD-ME and NADP-ME, respectively. The monomer molecular masses are 64 kDa for MaeA and 83 kDa for MaeB (Bologna *et al*., 2007). MaeA is involved in gluconeogenesis by providing pyruvate and has been used in metabolic engineering (Stols and Donnelly, 1997). However, the physiological function of MaeB has not yet been thoroughly analyzed. Recently, the kinetics of MeaA and MeaB were determined in detail (Bologna *et al*., 2007). Furthermore, the transcript profile of *E. coli* determined by using a DNA microarray revealed that *maeB* was up-regulated about 4 to 6-fold during growth on acetate compared with growth on glucose, which suggested that MaeB was involved in acetate metabolism (Oh *et al*., 2002). It was also proposed that MaeB may function as a generator of NADPH for *E. coli* growth when acetate is the sole carbon source (Zhu *et al*., 2005).

The present work was designed to characterize the biochemical properties of MaeB and its important physiological roles for acetate-grown *E. coli*. MaeB was overexpressed and purified from *E. coli* BL21 (DE3). The enzyme activity, optimum pH, optimum temperature and effects of metal ions were determined. Then, recombinant strains with a *maeB* deletion were constructed by homologous recombination, and their growth rates and MaeB activities in cells grown on different carbon sources were determined to investigate the physiological roles of MaeB in *E. coli*.

Materials and Methods

Bacterial strains and plasmids

E. coli MG1655 provided the wild type background for the experiments. *E. coli* DH5α was used as host for routine cloning. *E. coli* BL21(DE3) and vector pET28b(+) (Novagen) were used for protein expression. *E. coli* strains containing natural NADP-dependent IDH (icd^{NADP}) or engineered NAD-dependent IDH (icd^{NAD}) (Zhu *et al.*, 2005) were a gift from Antony M. Dean's laboratory (BioTechnology Institute, University of Minnesota, MN 55108, USA). Other plasmids used in this study were preserved in our laboratory.

Media and reagents

LB, SOB, SOC, and MOPS-based minimal medium were prepared as described elsewhere (Neidhardt *et al*., 1974; Stueland *et al*., 1988; Zhu *et al*., 2005). All media were supplemented with 100 μg/ml ampicillin, 15 μg/ml tetracycline, 30 μg/ml kanamycin, and 20 μg/ml chloramphenicol when necessary. Restriction enzymes and T4 DNA ligase were purchased from Sangon Biotech (China). PrimeStar™ HS DNA polymerase was obtained from TaKaRa (China). Plasmid and genomic DNA were extracted using Wizard® purification kits (Promega, USA). Proteins were purified using BD TALON ×Tractor Buffer and TALON Metal Affinity Resins (Clontech, USA). All primers were synthesized by Sangon Biotech (China).

Expression and purification of MaeB

The coding sequence of the *maeB* gene (GenBank database accession number AAC75516) was amplified by PCR from the genomic DNA of *E. coli* MG1655 with primers P1 and P2 (Table 1). A 2.2-kb product was then digested with *Nco*I and *Xho*I and ligated into pET-28b(+), creating pMaeB. The *E. coli* BL21(DE3) harboring pMaeB was cultured overnight in LB medium containing 30 μg/ml kanamycin at 225 rpm and 37°C. Cells were inoculated (1:100) into fresh LB medium until the culture density reached an OD_{600} of 0.5-0.6. The expression of MaeB was induced by adding isopropyl-β-D-thiogalactopyranoside (IPTG) to a final concentration of 10 μM for an additional 6 h of

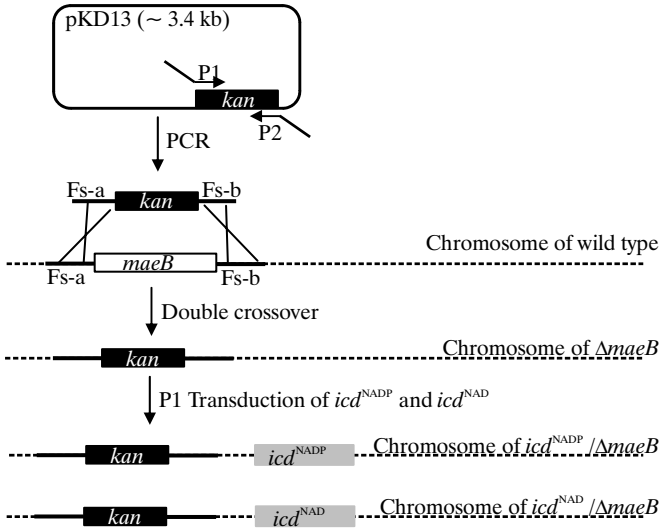

Fig. 1. Schematic illustration of the disruption of the *maeB* gene. The disruption of the *maeB* gene was done in wild type *E. coli* strain MG1655. Then the kan cassette was transduced using P1 (cml, clr100) into a fresh *E. coli* strain MG1655 background and the deletion of the *maeB* gene were confirmed by sequencing chromosomal PCR amplicons. Finally, the icd alleles (icd^{NADP} and icd^{NAD}) were cotransduced with the tet cassette into the Δ*maeB* background, resulting in icd^{NADP}/Δ*maeB* and icd^{NAD}/Δ*maeB* strains, respectively.
Abbreviations: kan, coding sequence of kanamycin; Fs-a, the upstream sequence of the *maeB* gene; Fs-b, the downstream sequence of the *maeB* gene.

cultivation. Cells were harvested and resuspended in BD TALON ×Tractor Buffer with 0.75 mg/ml of lysozyme and 2 U/ml of DNase. The debris was removed by centrifugation at 12,000 rpm for 20 min. Then, the 6His-tagged target protein in the supernatant was purified using BD TALON Metal Affinity Resins (Clontech) according to the manufacturer's instructions. The His-tagged enzyme was then desalted using buffer [100 mM Tris-HCl; pH 7.5, 10% (v/v) glycerol, and 20 mM β-mercaptoethanol] with GE Healthcare AKTA purifier. Enzyme purity was analyzed by 12% SDS-PAGE and stained with Coomassie Blue R250. Protein concentration was determined using the Bio-Rad protein assay kit (Bio-Rad) with bovine serum albumin as a standard.

MaeB activity assay

MaeB activity was determined spectrophotometrically at 30°C by monitoring NADPH production at 340 nm with a thermostated Cary 300 UV-Vis spectrophotometer (Varian, USA) (Detarsio *et al.*, 2004). The reaction mixture contained 50 mM Tris-HCl (pH 8.0), 20 mM $MnCl_2$, 0.5 mM $NADP^+$, 10 mM L-malate. One unit (U) of activity was defined as 1 μmol NADPH formed per min per mg of protein.

Determination of optimum pH, optimum temperature and effects of metal ions

The optimal pH for recombinant MaeB was determined in 50 mM Tris-HCl buffer over the range of pH 7.0-10.0. The optimal temperature tests were carried out at various temperatures from 25°C to 55°C. To investigate the effects of different metal ions, $MnCl_2$, $MgCl_2$, $CaCl_2$, $CuCl_2$, $ZnSO_4$, and $CoCl_2$ were added and MaeB activities were measured under the standard assay as described above.

Deletion of *maeB* gene by chromosomal homologous recombination

The *maeB* gene was knocked out using the phage λ recombination (Red) system (Datsenko and Wanner, 2000). A linear DNA fragment was amplified using a pair of 70-nt-long primers (D1 and D2) (Table 1) that included 50-nt homology extensions with the upstream (Fs-a) and downstream (Fs-b) sequences of the *maeB* gene and 20-nt priming sequences for the *kan* gene in template plasmid pKD13 (Fig. 1). The linear PCR product was introduced into competent *E. coli* MG1655 carrying pKD46 by $CaCl_2$ transformation (Johnson and Brooker, 1999). Cells were shocked at 42°C and recovered at 37°C in SOC, and then spread on LB plates to select kanamycin resistant transformants. The deletion of *maeB* was confirmed by sequencing the PCR products using primers C1-C5 (Table 1) whose regions spanned the flanking DNA on either side of the *kan* gene. The kan^r cassette replacing the *maeB* gene was transduced into a fresh *E. coli* MG1655 genetic background using P1 (*cml*, *clr100*), resulting in strain Δ*maeB*. The different genetic backgrounds containing either icd^{NADP} or icd^{NAD} were then introduced into Δ*maeB* by cotransduction with the tet^r cassettes. The resulting strains were denoted icd^{NADP}/Δ*maeB* and icd^{NAD}/Δ*maeB* (Fig. 1).

Activity analysis for recombinant strains

Each strain (30 ml culture) at exponential phase on different carbon sources was collected by centrifugation at 5,000 rpm for 15 min. The cells for each strain were washed twice in 1 ml of extraction buffer, containing 100 mM KH_2PO_4 (pH 7.0), 100 mM NaCl, 2 mM $MgCl_2$, 1 mM EDTA, 2 mM dithiothreitol (DTT), and 20% glycerol. After sonication for 10 min in an ice bath, the cell debris was removed by centrifugation at 12,000 rpm for 20 min at 4°C. Total MaeB activity was determined as described above.

Growth curve analysis

Strains were cultured in 25 ml of MOPS-based minimal medium containing 2% of either glucose or acetate as the sole carbon source

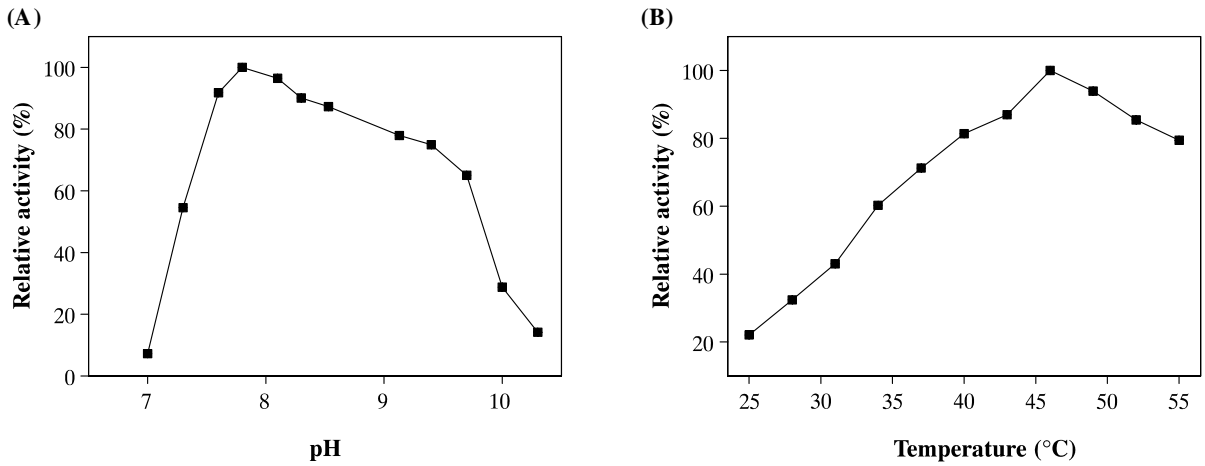

Fig. 2. The optimal pH (A) and temperature (B) profiles of the recombinant MaeB. (A) The effects of pH on the activity from pH 7.0 to 10.0. The pH stability is measured by incubating the purified MaeB at each pH at 46°C and assaying activity by monitoring NADPH production at 340 nm in the standard reaction mixture. (B) The effects of temperature on activity from 25°C to 55°C. The temperature stability is measured by incubating the purified MaeB at each temperature at pH 7.8 and assaying activity by monitoring NADPH production at 340 nm in the standard reaction mixture.

in a 250 ml flask at 37°C in an orbital shaker. Samples were taken every hour. The optical density was measured spectrophotometrically (UV-2102 spectrophotometer, UNICO Co. Ltd) at a wavelength of 600 nm in a cuvette with a 1 cm light path. The growth rates were calculated using the linear regression from logarithmic plots of the OD values at 600 nm versus time.

Results and Discussion

Expression of recombinant MaeB

A 2,200-bp PCR product was amplified from the *E. coli* MG1655 genome and cloned into pET-28b(+) vector. Then, MaeB was expressed as a 6His-tagged fusion protein. Consistent with conceptual translation of the MaeB open reading frame, SDS-PAGE suggested a molecular mass of approximately 83 kDa. Similar results have been obtained with two distinct malic enzymes from *Rhizobium meliloti* (82 kDa) (Mitsch *et al*., 1998; Voegele *et al*., 1999).

Table 2. Effects of metal ions on the activity of recombinant MaeB

Metal ions	Concentration (mM)	Relative activity (%)
None	−	15.35±1.22
Mn^{2+}	20	100.00±4.55
Mn^{2+}+Mn^{2+}	20+0.5	93.06±2.68
Mn^{2+}+Mg^{2+}	20+0.5	106.50±2.60
Mn^{2+}+Ca^{2+}	20+0.5	56.89±2.24
Mn^{2+}+Cu^{2+}	20+0.5	32.10±2.98
Mn^{2+}+Zn^{2+}	20+0.5	15.43±1.20
Mn^{2+}+Co^{2+}	20+0.5	79.72±2.46
Mg^{2+}	20	91.58±3.94
Mg^{2+}+Mg^{2+}	20+0.5	83.99±3.56
Mg^{2+}+Mn^{2+}	20+0.5	94.55±2.15
Mg^{2+}+Ca^{2+}	20+0.5	5.71±0.14
Mg^{2+}+Cu^{2+}	20+0.5	1.59±0.11
Mg^{2+}+Zn^{2+}	20+0.5	3.94±0.20
Mg^{2+}+Co^{2+}	20+0.5	1.86±0.08

Biochemical properties of MaeB

The optimal pH for recombinant MaeB was around pH 7.8 in the presence of Mn^{2+} (Fig. 2A), which is consistent with the reported result for MaeB from *E. coli* K-12 with Mg^{2+} (pH 7.5) (Bologna *et al*., 2007) under the same conditions. Maximum activity was observed at 46°C although the enzyme was rapidly inactivated above this temperature (Fig. 2B). The optimal activity of MaeB was 3.15 U/mg at pH 7.8 and 46°C.

The effects of various metal ions on MaeB activity were also examined (Table 2). We observed that the activity of recombinant MaeB was significantly dependent on the presence of a divalent cation. Mn^{2+} was found to be the most effective cation. Mg^{2+} could partially replace Mn^{2+}, resulting in approximately 92% of the maximal activity (Table 2). These results are similar to the previous report that the activity of malic enzyme from *Corynebacterium glutamicum* was dependent on the presence of divalent metal cations, especially Mn^{2+} and Mg^{2+} (Gourdon *et al*., 2000). In the presence of Mn^{2+}, the addition of Ca^{2+}, Cu^{2+} or Zn^{2+} reduced MaeB activity by 40%, 70%, and 80% of control value (Table 2) respectively. However, in the presence of Mg^{2+}, MaeB activity was dramatically inhibited by all four metal ions (Ca^{2+}, Cu^{2+}, Zn^{2+}, and Co^{2+}) being just 2-6% of the maximal activity (Table 2).

Table 3. Growth rates of *E. coli* mutants in various genetic backgrounds

Strain	Growth rate (h^{-1})	
	Glucose	Acetate
icd^{NADP}	0.67±0.03	0.35±0.02
icd^{NAD}	0.66±0.04	0.34±0.06
icd^{NADP}/Δ*maeB*	0.63±0.03	0.28±0.02
icd^{NAD}/Δ*maeB*	0.60±0.06	0.14±0.01

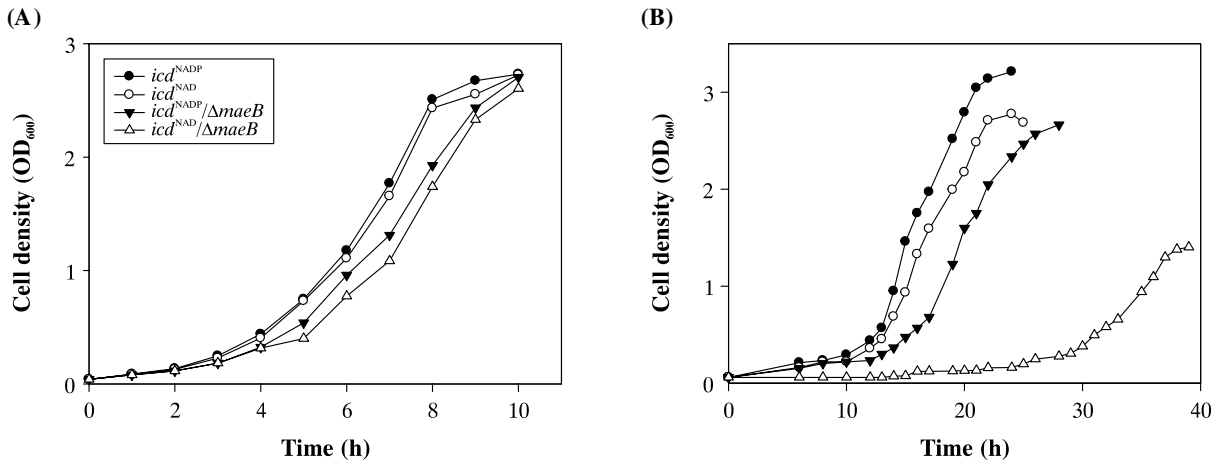

Fig. 3. Growth profiles of *E. coli* strains on glucose (A) or acetate (B). Strains were grown in 25 ml of MOPS-based minimal medium containing 2% of either glucose (A) or acetate (B) as a sole carbon source, in a 250 ml flask shaking at 200 rpm at 37°C. Cell densities were determined every h. Symbols: (■) icd^{NADP}; (●) icd^{NAD}; (□) icd^{NADP}/Δ*maeB*; (▼) icd^{NAD}/Δ*maeB*.

Effect of *maeB* deletion on bacterial growth

To explore the physiological role of MaeB, two deletion strains, icd^{NADP}/Δ*maeB* and icd^{NAD}/Δ*maeB*, were constructed by homologous recombination using *E. coli* MG1655 as the genetic background. The exponential growth of strains in various genetic backgrounds is presented in Table 3. There was no difference in the maximum growth rate between icd^{NADP} and icd^{NAD} during growth on glucose and acetate, which is consistent with the report described elsewhere (Zhu *et al*., 2005). We also did not observe a difference in the maximum growth rate between icd^{NADP}/Δ*maeB* and icd^{NAD}/Δ*maeB* during growth on glucose. However, when using acetate as a sole carbon source, icd^{NAD}/Δ*maeB* grew poorly and its growth rate was remarkably reduced (by 60%) as compared to the wild-type strain icd^{NADP} (Table 3). Additionally, icd^{NADP}/Δ*maeB* exhibited greater adaptability to acetate than icd^{NAD}/Δ*maeB*. Its growth rate was about 2-fold that of icd^{NAD}/Δ*maeB*, which may be due to more NADPH being generated by NADP-dependent IDH in icd^{NADP}/Δ*maeB*. These results suggested that MaeB was an important source of NADPH biosynthesis during growth on acetate.

Lag phase is an important period for bacterial adaptation to a new niche, which depends not only on the environmental conditions (temperature, pH, oxygen, and nutrient) but also on the cell density and cell viability. During adaptation to sequential use of glucose and acetate, these bacteria differentiate into two ecotypes that differ in their growth profiles. The 'slow-switcher' exhibits a long lag when switching to growth on acetate after depletion of glucose, whereas the 'fast-switcher' exhibits a short switching lag (Spencer *et al*., 2007). We observed that all strains grew well on glucose and displayed a similar lag phase (Fig. 3A). However, icd^{NAD}/Δ*maeB*, the 'slow-switcher', exhibited a very long switching lag as compared to the other three strains (Fig. 3B). Evidently, MaeB is an important factor for *E. coli* to adapt to acetate.

Table 4. MaeB activities of *E. coli* mutants in various genetic backgrounds

Strain	MaeB activity (U/mg)	
	Glucose	Acetate
Δ*maeB*	<0.01	<0.01
icd^{NADP}	0.45±0.03	0.82±0.03
icd^{NAD}	0.41±0.02	3.21±0.19

Effect of different carbon sources on MaeB activity

As shown in Table 4, the Δ*maeB* strains (icd^{NADP}/Δ*maeB* and icd^{NAD}/Δ*maeB*) had no detectable MaeB activity, while the icd^{NADP} and icd^{NAD} showed different activity during growth on different carbon substrates. During growth on glucose, MaeB activity was almost not affected by the coenzyme specificity of IDH. When switching to growth on acetate, MaeB activity was upregulated by 1.82-fold in icd^{NADP}, indicating that the enzyme may contribute to NADPH generation under stress conditions. Significantly, the activity of MaeB was enhanced by 7.83-fold in icd^{NAD}, which was about 3-fold higher than that in icd^{NADP} (Table 4). The marked increase of MaeB activity was probably induced by the absence of NADP-dependent IDH in the strain icd^{NAD}. In order to acquire necessary NADPH, icd^{NAD} initiated stress response mechanisms in bacteria to recruit NADPH from alternative pathways for biosynthesis, such as elevating MaeB activity. Furthermore, the balance in NAD(H)/NADP(H) ratio is critical for cell growth. The strain icd^{NAD}/Δ*maeB* may be incapable of reducing excess NADH production, which may cause an imbalance in the NAD(H)/NADP(H) ratio and result in its poor fitness on acetate. Thus, the physiological role of MaeB is to produce NADPH for bacterial adaptation to a poor carbon source, such as acetate.

In conclusion, we expressed and purified MaeB from *E. coli* MG1655. We then determined the biochemical properties of MaeB. The enzyme showed a maximum activity in the presence of Mn^{2+} and was strongly inhibited by Zn^{2+}. Furthermore, our results provide the first experimental evidence that MaeB activity was significantly enhanced during growth on acetate. It appears that MaeB is important for NADPH production

for bacterial growth on two-carbon compounds.

Acknowledgements

This work was supported by funds from the National Natural Science Foundation of China (30500300;30870062;31040003), the Natural Science Foundation of Anhui Education Department (KJ2010B352), the Key Science Project of Wuhu City (2009-4-7) and Program for Innovative Research Team in Anhui Normal University.

References

Bartolucci, S., R. Rella, A. Guagliardi, C.A. Raia, A. Gambacorta, M. De Rosa, and M. Rossi. 1987. Malic enzyme from archaebacterium *Sulfolobus solfataricus*. Purification, structure, and kinetic properties. *J. Biol. Chem.* 262, 7725-7731.

Bologna, F.P., C.S. Andreo, and M.F. Drincovich. 2007. *Escherichia coli* malic enzymes: Two isoforms with substantial differences in kinetic properties, metabolic regulation, and structure. *J. Bacteriol.* 189, 5937-5946.

Chang, G.G. and L. Tong. 2003. Structure and function of malic enzymes, a new class of oxidative decarboxylases. *Biochemistry* 42, 12721-12733.

Datsenko, K.A. and B.L. Wanner. 2000. One-step inactivation of chromosomal genes in *Escherichia coli* K-12 using PCR products. *Proc. Natl. Acad. Sci. USA* 97, 6640-6645.

Detarsio, E., C.S. Andreo, and M.F. Drincovich. 2004. Basic residues play key roles in catalysis and NADP(+)-specificity in maize (*Zea mays* L.) photosynthetic NADP(+)-dependent malic enzyme. *Biochem. J.* 382, 1025-1030.

Doležal, P., S. Vaňáčová, J. Tachezy, and I. Hrdý. 2004. Malic enzymes of *Trichomonas vaginalis*: two enzyme families, two distinct origins. *Gene* 329, 81-92.

Fukuda, W., Y.S. Ismail, T. Fukui, H. Atomi, and T. Imanaka. 2005. Characterization of an archaeal malic enzyme from the hyperthermophilic archaeon *Thermococcus kodakaraensis* KOD1. *Archaea* 1, 293-301.

Garrido-Pertierra, A., C. Martinez Marcos, M. Martin Fernandez, and M. Ruiz-Amil. 1983. Properties and function of malate enzyme from *Pseudomonas putida*. *Biochimie.* 65, 629-635.

Gourdon, P., M.F. Baucher, N.D. Lindley, and A. Guyonvarch. 2000. Cloning of the malic enzyme gene from *Corynebacterium glutamicum* and role of the enzyme in lactate metabolism. *Appl. Environ. Microbiol.* 66, 2981-2987.

Johnson, J.L. and R.J. Brooker. 1999. A K319N/E325Q double mutant of the lactose permease cotransports H+ with lactose - Implications for a proposed mechanism of H+ lactose symport. *J. Biol. Chem.* 274, 4074-4081.

Kobayashi, K., S. Doi, S. Negoro, I. Urabe, and H. Okada. 1989. Structure and properties of malic enzyme from *Bacillus stearothermophilus*. *J. Biol. Chem.* 264, 3200-3205.

Lamed, R. and J.G. Zeikus. 1981. Thermostable, ammonium-activated malic enzyme of *Clostridium thermocellum*. *Biochim. Biophys. Acta.* 660, 251-255.

Lance, C. and P. Rustin. 1984. The central role of malate in plant metabolism. *Physiol. Veg.* 22, 625-641.

Lerondel, G., T. Doan, N. Zamboni, U. Sauer, and S. Aymerich. 2006. YtsJ has the major physiological role of the four paralogous malic enzyme isoforms in *Bacillus subtilis*. *J. Bacteriol.* 188, 4727-4736.

Mitsch, M.J., R.T. Voegele, A. Cowie, M. Osteras, and T.M. Finan. 1998. Chimeric structure of the $NAD(P)^+$ - and $NADP^+$- dependent malic enzymes of *Rhizobium* (*Sinorhizobium*) *meliloti*. *J. Biol. Chem.* 273, 9330-9336.

Murai, T., M. Tokushige, J. Nagai, and H. Katsuki. 1971. Physiological functions of NAD- and NADP-linked malic enzymes in *Escherichia coli*. *Biochem. Biophys. Res. Commum.* 43, 875-881.

Neidhardt, F.C., P.L. Bloch, and D.F. Smith. 1974. Culture medium for enterobacteria. *J. Bacteriol.* 119, 736-747.

Oh, M.K., L. Rohlin, K.C. Kao, and J.C. Liao. 2002. Global expression profiling of acetate-grown *Escherichia coli*. *J. Biol. Chem.* 277, 13175-13183.

Sender, P.D., M.G. Martin, S. Peiru, and C. Magni. 2004. Characterization of an oxaloacetate decarboxylase that belongs to the malic enzyme family. *FEBS Lett.* 570, 217-222.

Seo, S.H., C.H. Rhee, and H.D. Park. 2007. Degradation of malic acid by *Issatchenkia orientalis* KMBL 5774, an acidophilic yeast strain isolated from Korean grape wine pomace. *J. Microbiol.* 45, 521-527.

Song, Y.D., J.P. Wynn, Y.H. Li, D. Grantham, and C. Ratledge. 2001. A pre-genetic study of the isoforms of malic enzyme associated with lipid accumulation in *Mucor circinelloides*. *Microbiology* 147, 1507-1515.

Spencer, C.C., M. Bertrand, M. Travisano, and M. Doebeli. 2007. Adaptive diversification in genes that regulate resource use in *Escherichia coli*. *PLoS Genet.* 3, 83-88.

Stols, L. and M.I. Donnelly. 1997. Production of succinic acid through overexpression of NAD(+)-dependent malic enzyme in an *Escherichia coli* mutant. *Appl. Environ. Microbiol.* 63, 2695-2701.

Stueland, C.S., K. Gorden, and D.C. LaPorte. 1988. The isocitrate dehydrogenase phosphorylation cycle. Identification of the primary rate-limiting step. *J. Biol. Chem.* 263, 19475-19479.

Suye, S.I., Y. Okada, A. Funada, M. Kawagoe, and S. Inuta. 1992. Purification and properties of malic enzyme from *Pseudomonas diminuta* IFO-13182. *J. Ferment. Bioeng.* 73, 343-347.

Voegele, R.T., M.J. Mitsch, and T.M. Finan. 1999. Characterization of two members of a novel malic enzyme class. *Biochem. Biophys. Acta.* 1432, 275-285.

Wheeler, M.C.G., M.A. Tronconi, M.F. Drincovich, C.S. Andreo, U.I. Flugge, and V.G. Maurino. 2005. A comprehensive analysis of the NADP-malic enzyme gene family of arabidopsis. *Plant Physiol.* 139, 39-51.

Zhu, G., G.B. Golding, and A.M. Dean. 2005. The selective cause of an ancient adaptation. *Science* 307, 1279-1282.